Longitudinal and lateral control for four wheel steering vehicles

Laëtitia Li, Brigitte d'Andréa-Novel, Arnaud Quadrat

Longitudinal and lateral control for four wheel steering vehicles

Laëtitia Li * **Brigitte d'Andréa-Novel** ** **Arnaud Quadrat** ***

* *Safran Electronics & Defense, 100 Avenue de Paris, 91344 Massy (e-mail: laetitia.li@safrangroup.com).*
** *Centre de Robotique, Mines ParisTech, PSL Research University, 60 boulevard Saint-Michel, 75272 Paris cedex 06, France (e-mail: brigitte.dandrea-novel@mines-paristech.fr)*
*** *Safran Electronics & Defense, 100 Avenue de Paris, 91344 Massy, (e-mail: arnaud.quadrat@safrangroup.com)*

Abstract: Vehicles evolving in harsh terrains are subject to physical phenomena with a much more important impact than in the case of road vehicle. The main problem we have to face is tire slippery which has to be taken into account when designing the control law to ensure an accurate tracking. In this paper we present a controller for cars equipped with 4 steering wheels. An accurate automatic trajectory tracking via vehicle wheel torque, front and rear steering is developed. This controller takes into account nonlinear tire effects to increase vehicle stability in presence of sliding. Promising results have been obtained with numerical simulations.

Keywords: Trajectory Tracking and Path Following, Autonomous Vehicles, Vehicle dynamic systems

1. INTRODUCTION

Most of the researches addressing the problem of automatic guidance of vehicles are based on two-wheel steering (2WS) vehicle, usually the front one, under rolling without sliding conditions [Thuilot (2004)]. This assumption is only valid for vehicles moving at low speed on adherent ground. Thus, for vehicles driving at relatively high speed on low grip conditions, numerous dynamic phenomena occur, mainly sliding effects, leading to tracking errors. Because the vehicles considered in this paper are expected to move on off-road conditions, sliding effects must be taken into account when designing the control law to preserve the tracking accuracy, regardless of the conditions of adherence, the path to follow and the nature of the ground. One solution consists in integrating sideslip angles when modelling the vehicle. However, 2WS vehicle only ensures the convergence of lateral deviation to zero. Indeed, angular deviation depends on road conditions and crabway motions are observed. To address this problem, [Cariou (2009)] used a four-wheel steering (4WS) vehicle and developed a controller based on a chained form [Samson (1995)] and backstepping approach, where both lateral and angular deviations can be explicitly controlled but they are regulated independently by the front and rear trains. Another solution consists in integrating a tire modelling taking into account tire/road interaction. Many researches about 4WS control have been carried out in this way and various control structures have been proposed in the literature using a wide variety of control techniques. Some of them try to increase the vehicle maneuverability during path following purpose in cluttered environment [Sekhavat (2000), Petrov (2009)] and suggest a control law where the rear steering angle is function of the front one. These approaches deprive those vehicles of the ability for crabwise motion and other asymmetrical steering modes. Others methods use dynamic feedback control algorithm [Yun (1996)], sliding mode control theory [Wang (2016), Hiraoka (2009)], for position and heading tracking errors. Many studies on 4WS vehicles also try to improve the vehicle handling performance and stability by tracking a reference yaw rate and slip angle by means of robust control techniques [Leith (2005), Wu (2007)], feedforward and feedback controller [Li (2009)], fuzzy controls strategy [Zhang (2007)] or optimal approaches [Amdouni (2013)]. In all previously mentionned methods, the vehicle orientation is held tangent to the reference path.

In this paper, trajectory tracking of a 4WS vehicle in presence of sliding is addressed. Adding a second steering axle, offers an additionnaly degree of freedom, allowing to control the vehicle orientation while following a path. The rear steering wheels are used to increase the stability of the vehicle by giving the vehicle the possibility of crabwise motion. A sliding steering axle will be compensated by the other one. The present paper presents a longitudinal/lateral nonlinear controller for 4WS vehicles where the position and orientation errors are both controlled by the three control following inputs : the wheel torque, the front and rear steering. The structure of the controller is based on a 3 Degrees of Freedom (DoF) bicycle dynamic model.

The rest of the paper is organized as follows: Section 2 defines the trajectory tracking problem. Section 3 presents the 3 DoF dynamic vehicle bicycle model. Then Section 4 describes the control algorithm for the trajectory tracking task based on backstepping approach. The effectiveness of the proposed controller is presented in section 5 via numerical simulation results based on a more realistic

9DoF vehicle model. Some concluding remarks and future works issues are given in Section 6.

2. TRAJECTORY TRACKING

Trajectory tracking aims at regulating the position and orientation of a vehicle towards a reference trajectory associated with a time law at a desired speed. It can be seen as regulating the vehicle, attached to a frame $[c] \triangleq (\boldsymbol{i}_c\ \boldsymbol{j}_c\ \boldsymbol{k}_c)$, towards a virtual vehicle, attached to a desired reference frame $[d] \triangleq (\boldsymbol{i}_d\ \boldsymbol{j}_d\ \boldsymbol{k}_d)$, which follows the ideal path. The configuration of the vehicle and the virtual vehicle, in the inertial frame $[i] \triangleq (\boldsymbol{i}_i\ \boldsymbol{j}_i\ \boldsymbol{k}_i)$, are respectively defined as $(X, Y, \psi)^T$ and $(X_d, Y_d, \psi_d)^T$. R_{ψ_d} is the transformation matrix between the frames $[d]$ and $[i]$ and R_ψ between the frames [c] and [i], such as:

$$R_\bullet \triangleq \begin{pmatrix} \cos(\bullet) & -\sin(\bullet) & 0 \\ \sin(\bullet) & \cos(\bullet) & 0 \\ 0 & 0 & 1 \end{pmatrix},$$

where $\bullet$ stands for ψ_d or ψ.
The trajectory tracking error (longitudinal, lateral and orientation errors), $e = (e_X, e_Y, e_\psi)^T$ in frame [i] and e_1 in frame $[c]$ are expressed as:

$$e_1 \triangleq R_{-\psi}\, e \quad \text{and} \quad \begin{cases} e_X \triangleq X_d - X, \\ e_Y \triangleq Y_d - Y, \\ e_\psi \triangleq \psi_d - \psi. \end{cases} \tag{1}$$

The following notations are taken : $x \triangleq (V_x, V_y, \dot{\psi})^T$ and $x_d \triangleq (V_{x_d}, V_{y_d}, \dot{\psi}_d)^T$ are respectively the true and the reference longitudinal and lateral speeds and yaw rates in the vehicle frame [c]. Differentiating e in frame [i] gives:

$$\dot{e} = R_{\psi_d}\, x_d - R_\psi\, x. \tag{2}$$

Projecting (2) into the vehicle frame gives :

$$e_2 \triangleq R_{-\psi}\, \dot{e} = R_{e_\psi}\, x_d - x. \tag{3}$$

The derivative of e_1 gives :

$$\Sigma_1 : \quad \dot{e}_1 = -\dot{\psi} \Lambda\, e_1 + e_2, \tag{4}$$

with

$$\Lambda \triangleq \begin{pmatrix} 0 & -1 & 0 \\ 1 & 0 & 0 \\ 0 & 0 & 0 \end{pmatrix}.$$

Finally, differentiating (3) one gets the error dynamics :

$$\Sigma_2 : \quad \dot{e}_2 = R_{e_\psi}(\dot{e}_\psi\, \Lambda\, x_d + \dot{x}_d) - \dot{x}. \tag{5}$$

3. THE 3DOF DYNAMIC BICYCLE MODEL

Because the vehicle considered in this paper could operate in a natural terrain, low grip conditions must be taken into account in the modeling to allow the design of accurate trajectory tracking laws. Thus 3DoF dynamical bicycle model which incorporates tire/ground interaction forces is considered here for the design of the controller. This model is obtained by reducing a four-wheel vehicle to a two-wheel vehicle, where the left and right wheel of each axle are lumped into a single wheel located at the center of the axle. This model assumes that the vehicle center of gravity height is low allowing to neglect the roll and pitch dynamics. The lateral dynamic is modeled in the yaw frame as depicted in Fig. 1 and notations are listed in Table 6. It is assumed that the 3DoF bicycle model is sufficient to describe the vehicle lateral dynamics.

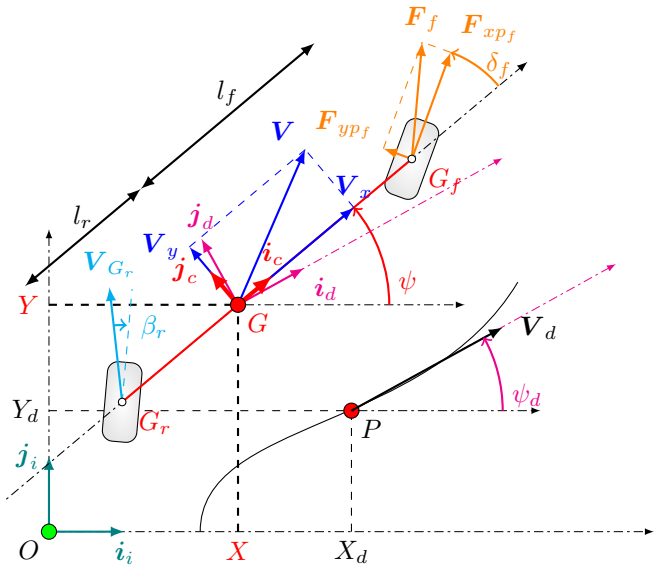

Fig. 1. Dynamic bicycle model

The 3DoF bicycle dynamic equations can be described as:

$$\begin{cases} m\,(\dot{V}_x - V_y \dot{\psi}) = F_{xf} + F_{xr}, \\ m\,(\dot{V}_y + V_x \dot{\psi}) = F_{yf} + F_{yr}, \\ I_z \ddot{\psi} = l_f\, F_{yf} - l_r\, F_{yr}. \end{cases} \tag{6}$$

The forces and moments of system (6) expressed in the vehicle frame $[c]$ are:

$$\begin{cases} F_{xf} = F_{xp_f}\, \cos\delta_f - F_{yp_f}\, \sin\delta_f, \\ F_{yf} = F_{yp_f}\, \cos\delta_f + F_{xp_f}\, \sin\delta_f, \\ F_{xr} = F_{xp_r}\, \cos\delta_r - F_{yp_r}\, \sin\delta_r, \\ F_{yr} = F_{yp_r}\, \cos\delta_r + F_{xp_r}\, \sin\delta_r. \end{cases} \tag{7}$$

with δ_f and δ_r the front and rear steering angles. In (7), the longitudinal forces are calculated using the dynamical model of the wheels:

$$\begin{cases} F_{xp_f}(\dot{\omega}_f) = \frac{p\, T_\omega - I_r\, \dot{\omega}_f}{r}, \\ F_{xp_r}(\dot{\omega}_r) = \frac{(1-p)\, T_\omega - I_r\, \dot{\omega}_r}{r}, \end{cases} \tag{8}$$

where p is a repartition coefficient of the total torque T_ω between front and rear wheels, and ranges from 0 (rear wheel drive) to 1 (front wheel drive), $\dot{\omega}_f$ and $\dot{\omega}_r$ are the wheels accelerations and $\dot{\omega} \triangleq (\dot{\omega}_f\ \dot{\omega}_r)^T$.

3.1 Dynamic bicycle model with linear tire model

With a linear tire force model, i.e considering lateral tire forces F_{yp} proportional to the sideslip angle $\beta \triangleq (\beta_f, \beta_r)^T$ where f stands for the front sideslip angle and r for the rear sideslip angle (see Fig. 1), the front and rear lateral forces are defined as follows [Rajamani (2012)]:

$$F_{yp} \approx F_{yp}^{\text{lin}} \triangleq C_\beta\, \beta,\ \beta \triangleq \delta - \begin{pmatrix} \frac{V_y + l_f \dot{\psi}}{V_x} \\ \frac{V_y - l_r \dot{\psi}}{V_x} \end{pmatrix},\ \delta \triangleq \begin{pmatrix} \delta_f \\ \delta_r \end{pmatrix},$$
$$F_{yp} \triangleq \begin{pmatrix} F_{yp_f} \\ F_{yp_r} \end{pmatrix},\ F_{yp}^{\text{lin}} \triangleq \begin{pmatrix} F_{yp_f}^{\text{lin}} \\ F_{yp_r}^{\text{lin}} \end{pmatrix},\ C_\beta \triangleq \begin{pmatrix} C_{\beta_f} & 0 \\ 0 & C_{\beta_r} \end{pmatrix}. \tag{9}$$

Considering small steering δ_f, δ_r angles assumption in (7) and by injecting (7), (8), (9) in (6), one gets:

$$\dot{x} = f(x, \dot{\omega}) + g(x, \dot{\omega})u + h(u), \tag{10}$$

where

$$f(x,\dot{\omega}) = \begin{pmatrix} V_y\dot{\psi} - \dfrac{I_r}{m\,r}(\dot{\omega}_f + \dot{\omega}_r) \\ -V_x\dot{\psi} - \dfrac{C_{\beta_f}(V_y + l_f\dot{\psi}) + C_{\beta_r}(V_y - l_r\dot{\psi})}{m\,V_x} \\ \dfrac{-l_f\,C_{\beta_f}(V_y + l_f\dot{\psi}) + l_r\,C_{\beta_r}(V_y - l_r\dot{\psi})}{I_z\,V_x}) \end{pmatrix},$$

$$u = \begin{pmatrix} T_\omega \\ \delta_f \\ \delta_r \end{pmatrix},\ h = \begin{pmatrix} -\dfrac{C_{\beta_f}\delta_f^2 + C_{\beta_r}\delta_r^2}{m} \\ \dfrac{p\,\delta_F\,T_\omega + (1-p)\,\delta_R\,T_\omega}{m\,r} \\ \dfrac{l_f\,p\,T_\omega\,\delta_F - l_r\,(1-p)\,T_\omega\,\delta_R}{r\,I_z} \end{pmatrix},$$

$$g(x,\dot{\omega}) = \begin{pmatrix} \frac{1}{m\,r} & \dfrac{C_{\beta_f}(V_y + l_f\dot{\psi})}{m\,V_x} & \dfrac{C_{\beta_r}(V_y - l_r\dot{\psi})}{m\,V_x} \\ 0 & \dfrac{r\,C_{\beta_f} - I_r\dot{\omega}_f}{r\,m} & \dfrac{r\,C_{\beta_r} - I_r\dot{\omega}_r}{r\,m} \\ 0 & \dfrac{l_f\,(r\,C_{\beta_f} - I_r\dot{\omega}_f)}{I_z\,r} & \dfrac{-l_r(r\,C_{\beta_r} - I_r\dot{\omega}_r)}{I_z\,r} \end{pmatrix}. \quad (11)$$

In order to reduce the complexity of the nonlinear model (10), nonlinear terms are neglected:

$$\dot{x} = f(x,\dot{\omega}) + g(x,\dot{\omega})\,u. \quad (12)$$

3.2 With nonlinear tire effects

The dynamic equations of the 3DoF model in the previous section is based on linear tire model but this assumption is only valid for small slip angles. For bigger slip angles, the lateral force F_{yp} generated by the tire is lower than the value given by the linear model $F_{yp}^{\text{lin}} = C_\beta\,\beta$ (see Fig.2). To take this error into account, the error terms $\widetilde{F}(\beta)$ are introduced, such as: $\widetilde{F} \triangleq F_{yp} - F_{yp}^{\text{lin}}$. Let us define the front or rear lateral force F_{yp} as being a function of the force F_{yp}^{lin} necessary for the trajectory tracking controller and the force $\widetilde{F}$ added for taking into account tires nonlinearities. Thus:

$$F_{yp} = F_{yp}^{\text{lin}} + \widetilde{F}, \quad (13)$$

$$\begin{cases} F_x \approx F_{xp} - \text{diag}(\delta)\,(\text{F}_{\text{yp}}^{\text{lin}} + \widetilde{\text{F}})\,, \\ F_y \approx (F_{yp}^{\text{lin}} + \widetilde{F}) + \text{diag}(\delta)\,\text{F}_{\text{xp}}. \end{cases} \quad (14)$$

Then, (6) gives :

$$\dot{x} = f_1(x,\dot{\omega}) + g_1(x,\dot{\omega})\,u, \quad (15)$$

with $f_1 \triangleq f + \Delta_f$, $g_1 \triangleq g + \Delta_g$, and

$$\Delta_g \triangleq \begin{pmatrix} 0 & -\widetilde{F}_f & -\widetilde{F}_r \\ 0 & 0 & 0 \\ 0 & 0 & 0 \end{pmatrix},\quad \alpha \triangleq \begin{pmatrix} 0 & 0 \\ \frac{1}{m} & \frac{1}{m} \\ \frac{l_f}{I_z} & \frac{-l_r}{I_z} \end{pmatrix},$$

$$\Delta_f \triangleq \begin{pmatrix} 0 & \frac{\widetilde{F}_f + \widetilde{F}_r}{m} & \frac{l_f\,\widetilde{F}_f - l_r\,\widetilde{F}_r}{I_z} \end{pmatrix}^T = \alpha\,\widetilde{F}. \quad (16)$$

4. CONTROL

4.1 Backstepping control design with linear tire model

One way for solving the trajectory tracking problem of a 4WS vehicle is through the expression of the dynamic error vector. By using (4) and (5), a control law based on backstepping technique can be designed. This controller globally asymptotically stabilizes the error.

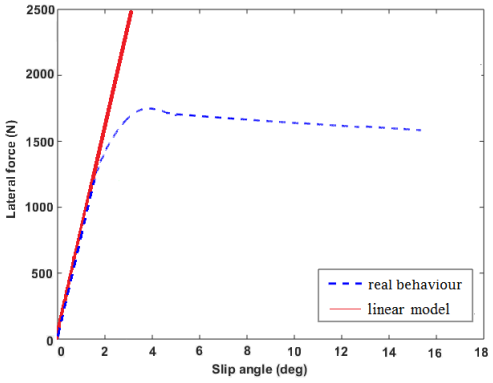

Fig. 2. Linear tire model VS nonlinear tire behaviour

Step 1 : At this step, (4) is considered and e_2 is seen as the control input of Σ_1. The goal is to regulate e_1 to zero. Thus, the first backstepping variable is chosen as : $z_1 \triangleq e_1$.

$$\Sigma_1 : \dot{z}_1 = -\dot{\psi}\Lambda z_1 + e_2. \quad (17)$$

The first Lyapunov candidate function is chosen as $V_1(z_1) \triangleq \frac{1}{2}z_1^T z_1$ and its derivative with respect to time is made negative by chosing $e_2 = \dot{\psi}\Lambda z_1 - K_1 z_1$, with K_1 a diagonal positive definite matrix, which leads to $\dot{V}_1(z_1) = -z_1^T K_1 z_1$. Since e_2 is not the real control input, the residual

$$z_2 \triangleq e_2 - e_{2d} \quad \text{with} \quad e_{2d} \triangleq \dot{\psi}\Lambda z_1 - K_1 z_1, \quad (18)$$

is introduced, allowing to stabilize Σ_1. Thus equation (17) is now $\dot{z}_1 = -\dot{\psi}\Lambda z_1 + z_2 + e_{2_d} = z_2 - K_1\,z_1$ and the Lyapunov derivative is $\dot{V}_1 = -z_1^T K_1 z_1 + \frac{1}{2}(z_2^T z_1 + z_1^T z_2)$.

Step 2 : A Lyapunov candidate function for z_2 dynamics, is $V_2 = V_1 + \frac{1}{2}z_2^T z_2$, which its derivative is

$$\dot{V}_2 = -z_1^T K_1 z_1 + \frac{1}{2}(z_2^T(z_1 + \dot{z}_2) + (z_1 + \dot{z}_2)^T z_2) \quad (19)$$

is made negative by chosing:

$$\dot{z}_2 = \dot{e}_2 - \dot{e}_{2d} = -z_1 - K_2\,z_2 \quad \text{with} \quad K_2 > 0, \quad (20)$$

giving $\dot{V}_2 = -z_1^T\,K_1\,z_1 - z_2^T\,K_2\,z_2 \leq 0$. The final control input is the vector u which appears in the term $\dot{x}$ (see (12) and (5)). By equalizing (20) and (5), the control law u regulating e_1 is obtained :

$$\begin{cases} u &= -g^{-1}\left(f - R_{e_\psi}(\dot{e}_\psi\,\Lambda\,x_d + \dot{x}_d) + U\right), \\ U &\triangleq \dot{e}_2 = \dot{e}_{2_d} - e_1 - K_2\,(e_2 - e_{2d}), \\ e_{2_d} &= \dot{\psi}\,\Lambda\,e_1 - K_1\,e_1, \\ \dot{e}_{2_d} &= \ddot{\psi}\,\Lambda\,e_1 + (\dot{\psi}\,\Lambda\, - K_1)\,\dot{e}_1. \end{cases} \quad (21)$$

Remark : the control law holds if g is invertible. It gives :

$$\det(g) = -\left(\frac{l_r(r\,C_{\beta_f} - I_r\,\dot{\omega}_f)(r\,C_{\beta_r} - I_r\dot{\omega}_r)}{m^2\,r^3\,I_z} + \frac{l_f\,(r\,C_{\beta_r} - I_r\,\dot{\omega}_r)(r\,C_{\beta_f} - I_r\dot{\omega}_f)}{m^2\,r^3\,I_z}\right), \quad (22)$$

$\frac{r\,C_\beta}{I_r}$ is around 10^4 and higher than the wheel rotation acceleration, then $r\,C_\beta - I_r\,\dot{\omega} \neq 0$.
Finally, the dynamic of the closed loop system is:

$$\begin{pmatrix} \dot{z}_1 \\ \dot{z}_2 \end{pmatrix} = \begin{pmatrix} -K_1 & 0 \\ 0 & -K_2 \end{pmatrix}\begin{pmatrix} z_1 \\ z_2 \end{pmatrix} + \begin{pmatrix} 0 & 1 \\ -1 & 0 \end{pmatrix}\begin{pmatrix} z_1 \\ z_2 \end{pmatrix}.$$

4.2 Backstepping control design with nonlinear feedforward compensations

Let us remind that the control law (21) designed in the previous section is based on linear tire model. In order to take into account the tires non-linearities, the system (15) is considered. The aim is to follow a reference trajectory while limiting the slip angles in order to prevent the vehicle from spinning and thus improving its controllability. This is made possible by taking advantage of the second steering axle. In such a case, the vehicle is able to follow the reference trajectory with any orientation as long as it is mechanically achievable. This behaviour will allow to reduce the vehicle side slip angles. Assuming that the contribution of the lateral forces in the longitudinal motion is negligible compared to the longitudinal forces, g_1 is now simplified in g. By noticing that $\widetilde{F}$ in (16) depends on the steering angles δ which are the control inputs, the terms $\bar{\Delta}_f$ are the delayed values of $\hat{\Delta}_f$ the estimation of Δ_f which will be determined below. Thus, one gets:

$$\begin{array}{l} \bar{\Delta}_f(s) \triangleq F_{LP}(s)\,\hat{\Delta}_f(s) = \alpha\, F_{LP}(s)\,\widehat{\widetilde{F}}(s), \\ F_{LP}(s) \triangleq \frac{1}{1+\frac{s}{2\,\pi\, f_0}},\ \widehat{\widetilde{F}} \triangleq \widehat{F}_{yp} - \widehat{F}_{yp}^{lin},\ \widehat{F}_{yp}^{lin} = \widehat{C}_\beta\,\beta, \end{array} \tag{23}$$

with, s the Laplace operator, $F_{LP}(s)$ a low-pass filter, f_0 the cut-off frequency. The terms $\widehat{\widetilde{F}}$ is calculated thanks to the method described in [Li (2019)]. The latter gives an estimation of the maximum lateral friction coefficient $\widehat{\mu}_{y_{\max}}$ and the cornering stiffness $\widehat{C}_\beta$ for the front and rear tires. As shown Fig. 3, the estimation is based on Inertial Navigation System measurements such as yaw rate $\dot{\psi}$, longitudinal V_x and lateral V_y velocities, longitudinal a_x and lateral a_y accelerations. We also need a measure of wheel torque T_ω and steering angles δ which are given by the computed control law itself and the wheel angular acceleration $\dot{\omega}$. The algorithm takes into account the linear and nonlinear part of tire characteristics by using a 3 zones adaptive algorithm. Once the estimated parameters $\widehat{C}_\beta$ and $\widehat{\mu}_{y_{\max}}$ have been obtained they are used in the Dugoff tire model [Rajamani (2012)] to get the estimated lateral forces $\widehat{F}_{yp}$:

$$\widehat{F}_{yp} \triangleq \begin{cases} \widehat{C}_\beta \tan(\beta) & \text{if } \lambda \geq 1 \\ \widehat{C}_\beta \tan(\beta)\,(2-\lambda)\lambda & \text{if } \lambda < 1 \end{cases} \tag{24}$$

and λ is given by: $\lambda = \dfrac{\widehat{\mu}_{y_{\max}} F_z}{2\,\widehat{C}_\beta \mid \tan\beta \mid}$.

Thus, a feedback control can be added to the control law (21) such as :

$$\begin{cases} u &= -g^{-1}\left(f - R_{e_\psi}(\dot{e}_\psi\,\Lambda\,x_r + \dot{x}_d) + U\right) \\ U &= \dot{e}_{2_d} - e_1 - K_2\,(e_2 - e_{2d}) - K_\Delta\,\bar{\Delta}_f, \\ e_{2_d} &= \dot{\psi}\,\Lambda\,e_1 - K_1\,e_1, \\ \dot{e}_{2_d} &= \ddot{\psi}\,\Lambda\,e_1 + (\dot{\psi}\,\Lambda - K_1)\,\dot{e}_1, \end{cases} \tag{25}$$

where $\ddot{\psi}$ is estimated with low-pass derivative filter. By imposing the control law as defined in (25), the Lyapunov candidate function defined in (19) is negative definite if

$$g_1 \approx g, \quad K_\Delta = \begin{pmatrix} 0 & 0 & 0 \\ 0 & k_y & 0 \\ 0 & 0 & k_\psi \end{pmatrix}, \quad k_y = -1, \quad k_\psi = -1.$$

However, for $g_1 \neq g$, $k_y > 0$ and $k_\psi > 0$ the system shows smaller slip angle β.

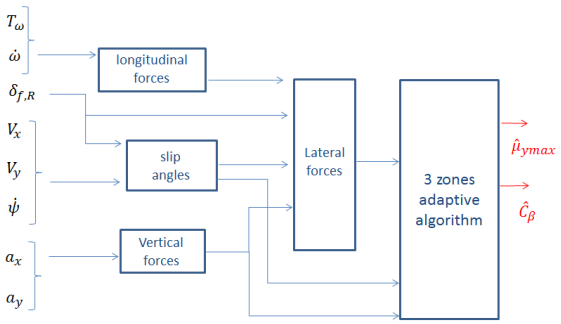

Fig. 3. $\hat{C}_\beta$ and $\hat{\mu}_{y_{max}}$ estimation

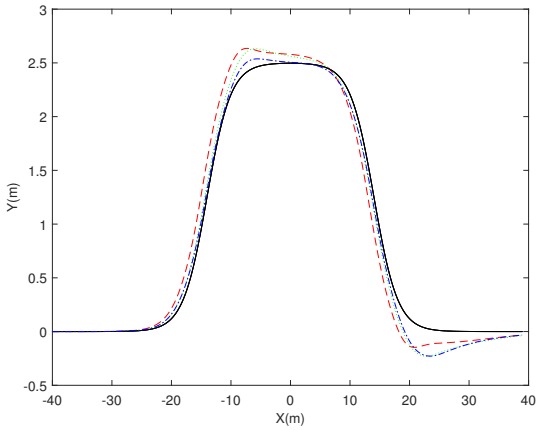

Fig. 4. Double lane change trajectory. Reference path (black solid line), trajectory tracking with (C1) (red dashed line), (C2) (green dotted line) and (C3) (blue dash-dotted line)

5. SIMULATION RESULTS

Numerical simulations (see Table-6 for numerical values) were performed to evaluate the effectiveness of the control law (25) with $k_y = 1$, $k_\psi = 1$ and are compared to the results obtained with (21). A 10 DoF vehicle model is used in order to simulate the vehicle dynamics $(V_x, V_y, V_z, \dot{\psi}, \dot{\theta}, \dot{\phi}, \omega_{fl}, \omega_{fr}, \omega_{rl}, \omega_{rr})$. The simulation integrates a Pacejka tire model the and numerical values are detailed in [Pacejka (2002)]. The control inputs of the simulator are the torque $T_{\omega_\bullet}$ applied at each wheel and the front δ_f and rear δ_r steering angles. In this work, a geometric reference trajectory and a desired travel speed V_d are given ($V_d = \dot{s}_d$, s being the curvilinear abscissa along the path). The desired reference velocities, V_{x_d},V_{y_d} and $\dot{\psi}_d$ are calculated based on the rolling without slipping assumption. In this case, the lateral speed at the center of gravity is zero and the reference yaw angle is tangent to the trajectory. The control algorithm was tested for a wet road condition such that the friction coefficient is $\mu_{y_{max}} = 0.8$. The car is following a double lane change trajectory as shown in Fig. 4, which is known as a benchmark test, involving the nonlinear dynamics of the tires and the car. Three simulations have been made. First, the control law (21) is applied and the cornering stiffnesses values are supposed to be unknown and are set to $3.10^4 N.rad^{-1}$ (this control law is called (C1) and will be displayed in red dashed curves). Then a second simulation

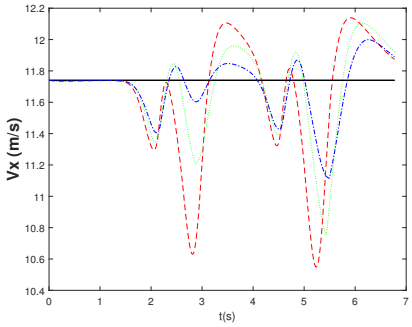

Fig. 5. Reference longitudinal speed (black solid line), V_x with (C1) (red), (C2) (green) and (C3) (blue)

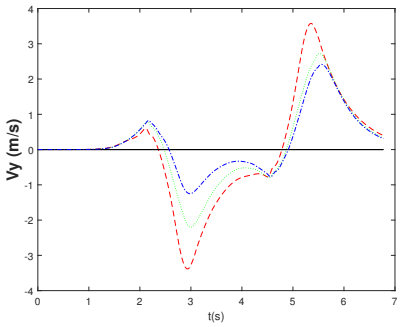

Fig. 6. Reference lateral speed (black solid line), V_y with (C1) (red), (C2) (green) and (C3) (blue)

is performed using (21) again but this time the cornering stiffnesses values are estimated with the method detailed in [Li (2019)] ((C2) displayed in green dotted curves). The last one simulation is performed with the control law (25) ((C3) displayed in blue dash-dotted curves). The cut-off frequency f_0 used in (25) is set to $20\,Hz$. The tuning of the diagonal matrices gains K_1 and K_2 remained the same for all the simulations and are set to 2 and 5 respectively. The parameter p is set to 0.5. The maximum curvature of the path is $\kappa = 0.057$, the maximum speed attainable is $V_d = \sqrt{\mu_{y_{max}}\, g/\kappa} = 11.74m/s$. At this speed, using (C1), the vehicle steering angles saturate as illustrated in Fig. 8 and Fig. 9, contrary to the ones obtained with (C2) and (C3). The front and rear lateral tire forces function of front and rear slip angles are depicted in Fig.11 and Fig.12. The tire behaviour reaches the nonlinear domain with (C1) whereas with (C2) and (C3) the tire tried to stay in the linear region and the tire slip angles are drastically decreased. This allows a better trajectory tracking as shown Fig.4, Fig. 5 and Fig. 6. The vehicle is able to follow the trajectory with accuracy and vehicle stability is increased thanks to an appropriate yaw orientation (Fig. 7). More simulations have been carried out and show, when using (C3), that the V_d speed can be increased up to $15m/s$ whereas the maximal attainable speed V_d with (C1) is $11.74m/s$.

6. CONCLUSION

The control law (21) allows to follow a path with an imposed yaw angle. Due to the assumption of linear tire model, this law is only consistent for small slip angles. Thus in slippery ground at high speed, the lateral tire forces saturate and the trajectory tracking is jeopardized.

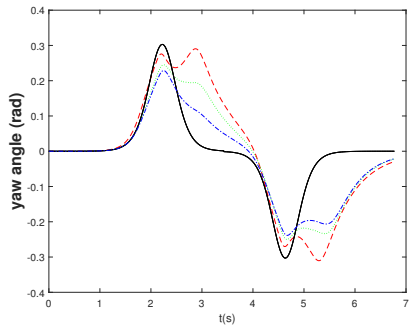

Fig. 7. Reference yaw angle (black solid line), ψ with (C1) (red), (C2) (green) and (C3) (blue)

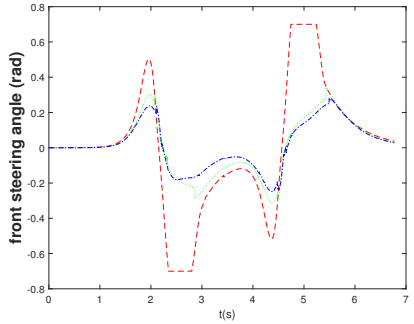

Fig. 8. Front steering angle with (C1) (red), (C2) (green) and (C3) (blue)

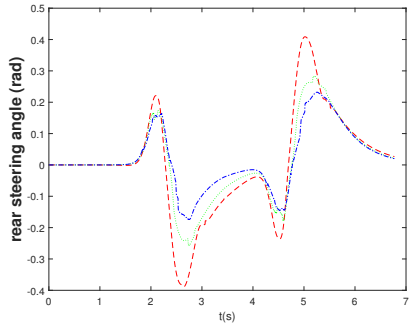

Fig. 9. Rear steering angle with (C1) (red), (C2) (green) and (C3) (blue)

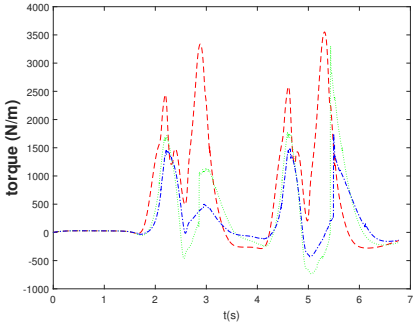

Fig. 10. Torque with (C1) (red), (C2) (green) and (C3) (blue)

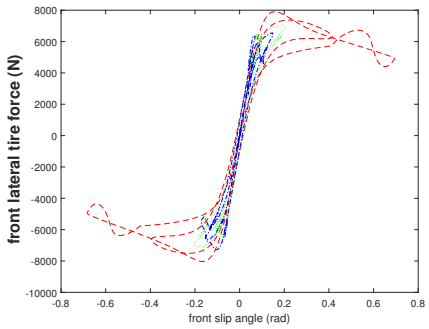

Fig. 11. Front lateral tire force function of front slip angle (with (C1) (red), (C2) (green) and (C3) (blue))

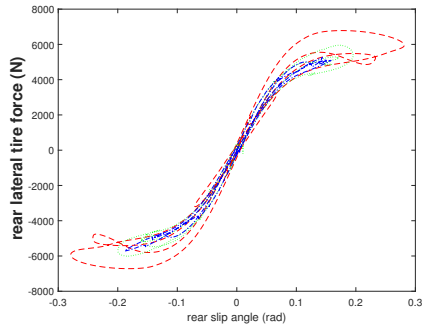

Fig. 12. Rear lateral tire force function of rear slip angle (with (C1) (red), (C2) (green) and (C3) (blue)

The rear steering angle brings an additional degree of freedom which allows to control the vehicle orientation. Thus, the proposed controller (25) tries to keep the tire in the linear region by influencing the yaw rate. For this purpose, a nonlinear tire force model is considered. The tire behaviour is caracterised by the knowledge of the cornering stiffness and the maximum lateral friction coefficient. These two parameters are obtained through an estimation algorithm detailed in [Li (2019)]. Promising results have been obtained and show a better trajectory tracking allowing to increase the travel speed.

REFERENCES

C.Samson. Control of Chained Systems Application to Path Following and Time-Varying Point-Stabilization of Mobile Robots. *IEEE Transactions on automatic control*, Vol. 40, No. 1, January 1995

B.Thuilot, J.Bom, F.Marmoiton, P.Martinet Accurate automatic guidance of an urban electric vehicle relying on a kinematic GPS sensor. *5th IFAC Symposium on intelligent autonomous vehicles*, 2004

C.Cariou, R.Lenain, B. Thuilot Automatic guidance of a four-wheel-steering mobile robot for accurate field operations. *Journal of Field Robotics, June*, 2009

S.Sekhavat, J.Hermosillo, The Cycab robot: A differentially flat systems, *Advanced Robotics,The Int. Journal of the Robotics Society of Japan*, 2000

P.Petrov, Nonlinear Path Following for a Bi-steerable Vehicle, *Information technologies and control*, 2009

X.Yun, S.Nilanjan Dynamic Feedback Control of Vehicles with Two Steerable Wheels, *Proceedings of the 1996 IEEE International Conference on Robotics and Automation Minneapolis*, April 1996

R.Wang, G.Yin, J.Zhuang, The Path Tracking of Four-Wheel Steering Autonomous Vehicles via Sliding Mode Control, *IEEE Vehicle Power and Propulsion Conference*, Oct. 2016

T.Hiraoka, O.Nishihara, H.Kumamoto, Automatic path-tracking controller of a four-wheel steering vehicle, *Vehicle System Dynamics*, Nov 2009

D.Leith, W.Leithead, M.Vilaplana, Robust lateral controller for 4-wheel steer cars with actuator constraints, *IEEE Conference on Decision and Control, and the European Control Conference*, 2005

B.Li, F.Yu, Optimal Model Following Control of Four-wheel Active Steering Vehicle, *Proceedings of the 2009 IEEE International Conference on Information and Automation* June 2009, China

J.Zhang, Y.Zhang, L.Chen, A fuzzy control strategy and optimization for four wheel steering system, *IEEE International Conference on Vehicular Electronics and Safety, ICVES* 2007

J.Wu, T.Houjun, S.Li, Improvement of vehicle handling and stability by integrated control of four wheel steering and direct yaw moment, *Proceedings of the 26th Chinese Control Conference* July 2007, China

I.Amdouni, N.Jeddi, L. El Amraoui, Optimal control approach developed to Four-Wheel Active Steering Vehicles, *5th International Conference on Modeling, Simulation and Applied Optimization* , 2013

L.Li, B. D'Andréa-Novel, S.Thorel, New online estimation algorithm of lateral tire-road coefficients based on Inertial Navigation System, *IEEE ITSC*, Auckland, October 2019

R. Rajamani Vehicle Dynamics and Control, *Springer*, 2012.

H.B. Pacejka, Tyre and Vehicle Dynamics. *Butterworth-Heinemann*, 2002

Table 1. Vehicle parameters

G	gravity center
δ_f, δ_r	front and rear steering angle
m	vehicle mass : 1878 Kg
I_z	yaw moment of inertia : 4045 Kg.m^2
l_f (l_r)	distance from front (rear) axle to G : $l_f = 1.3$m, $l_r = 1.8$m
$\psi(\psi_d), \dot{\psi}(\dot{\psi}_d), \ddot{\psi}(\ddot{\psi}_r)$	actual (desired) yaw angle, rate and acceleration
$\dot{\theta}$, $\dot{\phi}$	roll and pitch rates
$V_x(V_{x_d}), \dot{V}_x(\dot{V}_{x_d})$	actual (desired) longitudinal speed and acceleration in the vehicle frame
$V_y(V_{y_d}), \dot{V}_y(\dot{V}_{y_d})$	actual (desired) longitudinal speed and acceleration in the vehicle frame
I_r	wheel moment of inertia : 1.3 Kg.m^2
r	tire radius : 0.34m
$F_{x_f}(F_{y_f}), F_{x_r}(F_{y_r})$	front and rear longitudinal (lateral) tire force (car frame)
$F_{xp_f}(F_{yp_f}), F_{xp_r}, (F_{yp_r})$	front and rear longitudinal (lateral) tire force (wheel frame)
β_r, β_f	rear and front slip angle
C_{β_r}, C_{β_f}	rear and front cornering stiffness
$\mu_{y_{max}}$	maximum lateral friction coefficient
$T_\omega, T_{\omega_f}, T_{\omega_r}$	total, front and rear wheel torque
p	torque repartition coefficient
$\dot{\omega}_f, \dot{\omega}_r$	front and rear wheels rotation acceleration
$R_\psi, R_{\psi_d}, R_{e_\psi}$	rotation matrix
K_i	gains